

XPS Valence Band Study of Zeolites and Related Systems. 1. General Chemistry and Structure

Tery L. Barr,^{*,†,‡} Li Mei Chen,[‡] Mehran Mohsenian,[‡] and Marie A. Lishka[§]

Contribution from the Department of Materials and Laboratory for Surface Studies, University of Wisconsin—Milwaukee, P.O. Box 784, Milwaukee, Wisconsin 53201, and Allied-Signal Engineered Materials Research Center, Des Plaines, Illinois 60017-5016.

Received October 30, 1987

Abstract: The first detailed, reproducible, experimental results are presented of the valence band spectra of a variety of commercially important zeolites. These were obtained using X-ray photoelectron spectroscopy (XPS or ESCA). A general *chemical* formulation of $(\text{SiO}_2)_x \cdot (\text{M}^{+p})_{1/p} \text{AlO}_2^-)_y \cdot \text{ZH}_2\text{O}$ applies to the materials examined, where, for most of the cases studied herein, $\text{M}^{+p} = \text{Na}^+$. Comparisons are made with well-known experimental and theoretical (MO and band structure) results for various silicas and aluminas. Numerous interrelationships are found involving most of the key subband features documented for the latter materials. Distinct shifts and truncations are found in the zeolite bands. These suggest that zeolites more closely depict an agglomeration than a persistent type mixture of the aforementioned precursors. Analyses demonstrate that many of these features and changes seem to key on the ratio of x to y in the aforementioned chemical formulation, in a manner similar to that reported in our previous core level XPS studies. Results are also presented that suggest distinct detectable valence band differences that reflect major changes in the critical structures of these materials. In particular, we herein suggest the use of XPS valence bands as a means to determine novel groupings into (I) primarily cage-like zeolites (e.g., A, faujasites, and L) and (II) primarily chain-like (e.g., mordenite, ZSM-5, and silicalite) structures. Additional valence band studies involving cation changes, use and abuse of these systems, and comparisons with valence bands of similar oxides (e.g., Ga_2O_3 and GeO_2) are reported elsewhere.

I. Introduction

A. Generalities. Zeolites exhibit numerous, very complex structures of both natural and synthetic origin. Their many important industrial uses are promoted, in part, by the regularity and size of the channels formed by their lattices, and also by the dramatic variety of charge fields (usually acidic in nature) that may be realized by changing the type and position of the ions that balance the charges inherent to these lattices.¹

All of this has contributed to produce a fertile area for materials characterization, as well as synthesis. In fact, characterizations have played pivotal roles in the development of this field for more than 25 years.¹ Most of these analyses have centered on the bulk aspects of these materials, with zeolite surfaces, despite their potential importance, receiving far less productive attention. Fortunately, recent efforts seem to be remedying this disparity, with very useful studies being rendered using fast atom bombardment mass spectrometry (FABMS),² Auger,³ X-ray photoelectron spectroscopy (XPS or ESCA)⁴ and even adroit mixed bulk-surface approaches, particularly by Suib et al.⁵

Over the last few years, novel studies performed in our laboratories have demonstrated the use of ESCA as a means to monitor a variety of important surface features of various zeolites, and also to relate those features to those detected in moieties that may be viewed as quasi-zeolite precursors, e.g., silicas, aluminas, etc.^{4,6-8} These studies have included the first detection of a set of characteristic core level binding energy shifts for the zeolites and other species that seem to depend, in a unique manner, on both the [Si/Al] ratios (note that we are, at present, restricting our consideration to only Si—Al molecular sieves) and the type and charge of the associated cations, M^{+p} . We will hereafter describe the zeolites of interest through a general, compositional formula $(\text{SiO}_2)_x \cdot (\text{M}^{+p})_{1/p} \text{AlO}_2^-)_y$.⁷ It was also suggested that part of the detected shifts may be dependent upon the structure of the zeolites under study, e.g., faujasites, A type, etc.^{7,8}

In addition to the core level chemical shifts, a number of additional variable parametric features were discovered (for relatively pure species), including interesting, repetitive patterns of surface composition that are apparently induced when these systems are

sputter etched with selected energies of relatively monoenergetic argon ions.⁷ This observation is of potential importance because the damage realized during sputtering is so selective and repetitive it may actually be employable as a supplementary, qualitative, detective tool to identify presputtered compositions, and also provide useful information about bonding, relative stability, and other key features, particularly, as we shall show, in relationship to certain key deleterious stages in catalytic use of these moieties.⁹

Recently we have extended these studies to include the utilization of the aforementioned shifting patterns as a means to detect and identify surface oriented byproducts and impurities found in different zeolite matrices. Thus, for example, extensive Al_2O_3 and metal aluminate species were detected at the surface of freshly prepared (supposedly pure) mordenite, silicalite, and ZSM-5.⁸ (The interesting similarity between the appearance of the Al(2p) peaks reported in that study and ours should be noted.) The potential importance of this type of study should be obvious, since areas of zeolite utilization such as catalysis may be markedly affected by the presence of some of the byproducts detected, e.g., the relationship between the presence of aluminas and coke formation.¹⁰ An example of the direct use of ESCA as a useful, perhaps unique, tool for zeolite catalysis studies is presented in a succeeding paper (hereafter referred to as Zeo VIII).⁹

(1) (a) Breck, D. W. *Zeolite Molecular Sieves*; New York, 1974. (b) Rabo, J. A., Ed.; *Zeolite Chemistry and Catalysis*; American Chemical Society: Washington, D.C., 1976; Monograph Ser. No. 171.

(2) See, for example: Dwyer, J.; Fitch, F. R.; Quin, G.; Vickerman, J. C. *J. Phys. Chem.* **1982**, *86*, 4574.

(3) See, for example: Suib, S. L.; Stucky, G. D.; Blattner, R. J. *J. Catal.* **1980**, *65*, 174, 179. Suib, S. L.; Coughlin, D. F.; Otter, F. A.; Conopaski, L. F. *Ibid.* **1983**, *84*, 410.

(4) For a recent review, see: Barr, T. L. In *Practical Surface Analysis by Auger and Photoelectron Spectroscopy*; Briggs, D., Seah, M. P., Eds.; Wiley: New York, 1983; Chapter 8.

(5) See, for example: Suib, S. L.; Kostapapas, A.; Psaras, D. *J. Am. Chem. Soc.* **1984**, *106*, 1614. Suib, S. L.; Kostapapas, A. *Ibid.* **1984**, *106*, 7705. Morrison, T. I.; Iton, L. E.; Sheney, G. K.; Stucky, G. D.; Suib, S. L.; Reis, A. H., Jr. *J. Chem. Phys.* **1980**, *73*, 4705. Suib, S. L.; McMahon, K. C.; Psaras, D. *Intra-Zeolite Chemistry*; ACS Symp. Ser. **1983**, No. 218, 301.

(6) Barr, T. L. *ACS Div. Petrol. Chem.* **1978**, *23*, 82.

(7) Barr, T. L. *Appl. Surf. Sci.* **1983**, *15*, 1.

(8) Barr, T. L.; Lishka, M. A. *J. Am. Chem. Soc.* **1986**, *108*, 3178.

(9) Barr, T. L.; Chen, L. M.; Mohsenian, M.; Lishka, M. A. *J. Catal.*, to be submitted for publication.

(10) See, for example: Emmett, P. H.; Sabatier, P. *Catalysis Then and Now*, Franklin: Englewood, N. J., 1965.

* To whom correspondence should be addressed.

[†] Formerly at the Allied-Signal Engineered Materials Research Center, where much of the experimental work was accomplished.

[‡] University of Wisconsin.

[§] Allied-Signal Engineered Materials Research Center.

In this and several subsequent publications we will expand upon studies of silica-aluminate systems employing another area of X-ray induced ESCA that was also initially reported, in a preliminary fashion in references Zeo II-IV.^{4,7,8} The feature of ESCA under consideration is the generation of *valence band spectra*. Because of the nature of the bands for the materials in question, we will restrict our observations to the binding energy regions from 0 to 20 eV. This will permit us to monitor the bands that can be reasonably depicted as formed from the involvement of Si and Al(3s and 3p) and O(2p) orbitals. Comparisons are also made with selected calculations of similar features, although in the present case we omit those peaks at ~23 eV that are primarily formed from O(2s) orbitals, and sometimes considered to be part of the valence band.

It should be noted that, because of the relatively large kinetic energy of the resulting photoelectrons (of the order of 1460 eV for spectra generated with Al K α X-rays), the sampling depths for the reported studies may be significantly greater than those realized in studies of similar materials employing UV or low-energy synchrotron radiation. This enhanced depth is an advantage that permits us generally to analyze below any extraneous outer surface damage that may exist on these commercially prepared materials, and thus detect sufficient features of the true zeolite lattices. In these relatively practical instances, this feature may more than compensate for the somewhat enhanced resolution often realized with less energetic photoelectron beams. If one compares results achieved using different energy sources, one must, of course, remember also to take into consideration the often extreme differences realized in photoelectron cross sections. Even other XPS results, such as those designed to generate relative quantitation employing O(1s) lines, should be compared with the present results with great caution.

It should be noted that all of the discussions contained herein are based upon arguments that ignore distinctions between initial- and final-state photoelectron effects. It is well known, however, that the most substantial contributions to final-state loss (relaxation-type) processes require the presence of deep (localized) holes. For this reason final-state shifts are generally small for valence band photoelectrons, although moderate extranuclear relaxation shifts may occur in wide band gapped oxides due to localized valence band holes. The latter and many of the other small, but nonzero, effects should effectively cancel in the following largely qualitative, comparative analysis. For this reason, we will assume that all measured results as utilized herein can be referred to initial state (e.g., covalency/ionicity) properties.

In this paper (Zeo V), we will present and analyze the valence band spectra for a series of zeolites, and also several of the aforementioned precursor systems. The reproducibility of these results will be considered in detail, as this is an important aspect of these studies. The data will include evidence for shifts in both band position and size, and these will be shown to correlate with changes in fundamental features (e.g., [Si/Al] and structure) for these zeolites. Special consideration is also given to how these ESCA results compare to a hypothetical "composition model" that we have proposed for these zeolite systems. Finally, we will suggest the potential utility of these observations as a separate means to monitor the surface integrity of silica-aluminate systems and also any purposefully induced modification. Several demonstrations of the latter capability will be presented in a succeeding paper, Zeo IX.¹¹

B. Designations. In order to begin these studies, there are several difficult and somewhat imprecise points of nomenclature that need to be clarified. In particular, it should be noted that there are a wide variety of structural and chemical entities that are often labeled silicas, Al₂O₃, zeolites, etc. It is not uncommon, for example, for some researchers to describe properties and uses for a material that is primarily a boehmite (AlOOH) and yet to label it as Al₂O₃. Part of this problem arises from the need and difficulty involved in achieving descriptive generality. We face

the same problem and will address it in the following useful (but imprecise) manner:

(1) All Al_xO_yH_z systems will be collectively labeled as *aluminas*, even if $z \neq 0$. (2) All Si_xO_yH_z systems will correspondingly be called *silicas*. (3) All materials generally designated as *zeolites* may be assumed to be crystalline molecular sieves with the general (chemical) formulation: (SiO₂)_x · (M^{+p}_{1/p}AlO₂)_y · zH₂O with only silicon, aluminum, and oxygen in the highly porous, large crystalline lattice structures. The other species M^{+p} and H₂O are assumed to be interfaced throughout these lattices to achieve proper charge and material balance. (Note that results will be presented in a later series of papers concerning molecular sieves with other components, e.g., P in their lattice structure.) (4) Several other silica-aluminates or alumina silicates have been examined and will be reported in subsequent papers. These will be described as clays and assumed generally to represent the ESCA features of a small segment of that type of material.

II. Experimental Section

A. Materials Examined. The materials featured in this study were obtained from common outside commercial suppliers. All were purported to have excellent composition and structural integrity. These materials were obtained as fine mesh powders and were all (lightly) pressed into thin (relatively) smooth cylindrical wafers in the specially designed HP ESCA platens. The details of their physical and chemical status before and during examination have been described elsewhere.⁶⁻⁸

B. Analysis Equipment. Most of the surface studies were conducted with a Hewlett-Packard (HP) 5950A ESCA spectrometer. Those features of this system that are key ingredients in these analyses have been described elsewhere in some detail;¹² therefore, these descriptions will not be repeated herein. It should be noted that both the resolution and stability of the HP system and the conventional (HP 18623A) electron flood gun played the same integral roles in the present analyses. All readers interested in the mechanics of these examinations should consult the other publications for the methodology employed to remove the charging shift inherent to all these systems and also the resulting lack of a fixed Fermi edge.^{4,7,8,13,14} Unless stated otherwise, the reported binding energies for the silica-aluminate systems exhibited a *precision* of $\Delta BE = \pm 0.15$ eV.

The HP-ESCA system was employed at an analyzer pressure of $\sim 1 \times 10^{-9}$ torr. The temperature in the analyzer chamber was maintained at ~ 25 °C. The soft nature of the monochromatized Al K α X-rays produced no materials damage that could be detected by the ESCA.

In addition, several valence band spectra were generated using a Leybold-Heraeus (LH) ESCA (at the University of Connecticut under the supervision of Professor S. L. Suib) and a Physical Electronics (PHI) system (at the PHI Analysis Laboratory, Eden Prairie, Minn.). These measurements were performed on zeolite materials different from those studied with the HP system. Because of reduced scan time and lack of a monochromator, some of these analyses do not reveal the same detailed features as those achieved with the HP. They are included in the present study, however, because the general features that are detected are identical with those obtained with the HP, thus arguing for the generality of the reported results.

III. Review of the Important Valence State Calculations

To our knowledge there are no detailed valence electronic (band structure) calculations of zeolites. Recently, there have been several reasonably elaborate molecular cluster calculations¹⁵ of zeolites, primarily with the goal of describing zeolite adsorption, rather than its general internal bonding and band structure. These theoretical studies have demonstrated some success in modeling various Si-O-Si, Si-O-Al, and even Al-O-Al bonding environments.^{15b,16} These seem to pertain directly to certain structural features, selective adsorption sites,¹⁷ the Lowenstein rule argument,¹⁵ and the very important consideration of the contributions of hydroxyl-type bonds and aluminum coordination to acidity.^{15b,18}

(12) Barr, T. L. *Am. Lab.* **1978**, *10*, 40, 65.

(13) Barr, T. L.; Kramer, B.; Shah, S. I.; Ray, M.; Greene, J. *Mater. Res. Soc. Proc.* **1985**, *47*, 205.

(14) Kao, C. C.; Merrill, R. P.; Barr, T. L., to be published. Barr, T. L.; Kao, C. C., to be published.

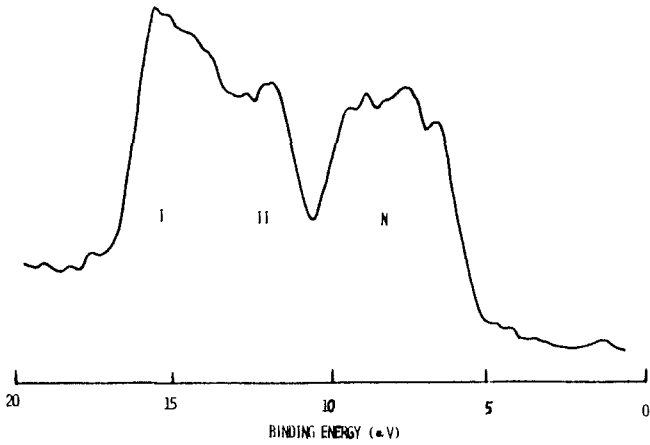
(15) (a) Sauer, J.; Zahradnik, R. *Int. J. Quantum Chem.* **1984**, *25*, 793.

(b) Derouane, E. G.; Fripiat, J. G. *J. Phys. Chem.* **1987**, *91*, 145.

(16) Sauer, J.; Engelhardt, G. *Z. Naturforsch., Ann.* **1982**, *37*, 277.

(17) Sauer, J.; Habza, P.; Zahradnik, R. *J. Phys. Chem.* **1980**, *84*, 3318.

(11) Barr, T. L.; Chen, L. M.; Lishka, M. A. *Zeolite*, to be submitted for publication.

Table I. Representative Selected Sub-Band Maxima and Minima Points and Key Differences for Silicas and Silica-like Systems (in eV ± 0.25)


Part A							
	0	A	B	C	D	E	5
α -silica	16.7	15.3	11.7	10.4	7.8	6.4	5.0
silica gel	16.1	13.8	10.6	8.9	6.8	5.6	3.3
silicalite	15.8	14.3	10.9	9.2	7.0	5.4	3.5
ZSM-5	16.5	14.7	11.2	9.5	7.5	6.0	3.3
mordenite	15.7	13.7	10.5	9.1	7.0	5.8	3.3

Part B									
	0-5	0-A	A-C	A-D	A-E	C-E	B-D	B-E	E-5
α -silica	11.7	1.4	4.9	7.4	8.9	4.0	3.8	5.3	1.4
silica gel	12.8	2.3	4.4	7.0	8.2	3.3	3.8	5.0	2.3
silicalite	12.3	1.8	4.8	7.0	8.6	3.8	3.9	5.5	1.9
ZSM-5	12.8	1.75	5.25	7.25	7.75	3.5	3.7	5.2	2.3
mordenite	12.4	2.0	4.6	6.7	7.9	3.3	3.5	4.7	2.5

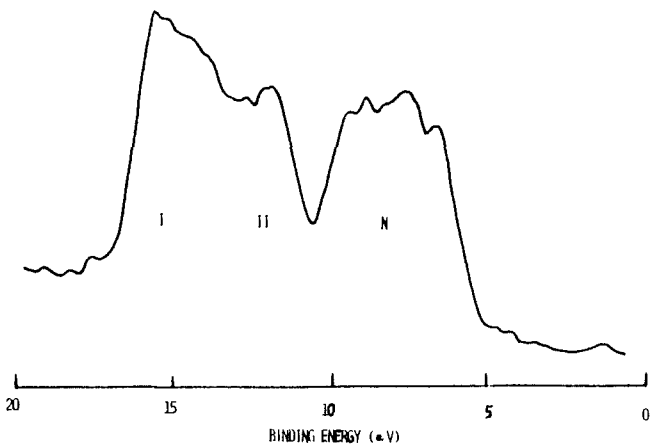
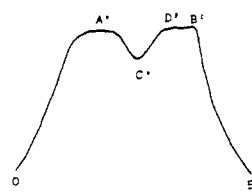
Although perhaps only indirectly impacted by the present experimental study, it is obvious that these calculations will play a significant role in our future research program where hydration, acidity, adsorption, etc., will be major concerns.

There are also relatively few detailed calculations of the valence structure of silicas and aluminas. Those that do exist have primarily concentrated on various studies of SiO_2 , ranging from the molecular orbital results of Pantelides¹⁹ and others,²⁰ to the SCF- $X\alpha$ values computed by Tossell,²¹ plus the detailed band structure calculations of, for example, Fowler et al.,²² Chelikowsky et al.,²³ Batra et al.,²⁴ and Joannopoulos et al.²⁵ The less numerous alumina and aluminate calculations have included a SCF- $X\alpha$ study by Tossell,²⁶ and the band theory results of Batra²⁷ and Ciraci and Batra.²⁸ Recent studies have attempted to broaden the scope of this area by including such important auxiliary effects as hydration,²⁹ but the bases employed in the latter examinations were rather sparse.

The efforts by Tossell^{21,26} are particularly useful to us in the present study, because he performed his calculations on the aluminate system forced into a tetrahedral (rather than the more typical hexagonal) environment. This permits a more direct comparison with the tetrahedral zeolite results. Batra's band structure results^{24,27,28} are also very illuminating because he was particularly concerned with the relationship between silica and alumina systems, often commenting on the bonding/nonbonding order and the splitting and also the relative degree of ionicity.

Although available in detail elsewhere, it is of importance to reconsider here some of the key achievements of these calculations.

1. The silica band structure is, on the whole, rather broad (~ 10 eV) (see Table I) with readily apparent delineation into three

**Figure 1.** Representative valence band spectrum for $\alpha\text{-SiO}_2$.**Table II.** Representative Selected Sub-Band Maxima and Minima Points and Key Differences for Alumina Systems (in eV ± 0.25)


Part A						
	0	A'	C'	D'	E'	5
α -alumina	13.5	9.9	8.0	6.7	5.8	2.3
γ -alumina	13.3	9.8	7.5	6.2	4.8	2.7

Part B							
	0-5	0-A'	A'-C'	A'-D'	A'-E'	C'-E'	E'-5
α -alumina	11.2	3.6	1.9	3.2	4.1	2.2	3.5
γ -alumina	10.6	3.5	2.3	3.6	5.0	2.7	2.1

subbands. The first (N), Figure 1, is ~ 4.5 eV in width (measured across the top of the subband) and at lower binding energy than the balance of the structure. It is primarily formed from O(2p) nonbonding orbitals. There may even be some π character in this subband. The second region (II) is readily split from the first by a nonoverlapping density chasm that is more than 1 eV in width. This gulf is the bonding "barrier" for silica. The relatively narrow second subband region (II) is formed primarily from Si(3p) stabilized (bonding) O(2p) orbitals. The actual contribution of Si(3p) to the density in this region is much less than O(2p), but still finite. There may be an apparent gap between this second and the third band region (I), with the latter apparently formed from the (σ bonding) stabilization of O(2p) orbitals primarily by Si(3s). This apparent gap is suggested in the SCF- $X\alpha$ calculations of Tossell,²⁶ and has been observed in the XPS valence band studies of $\alpha\text{-SiO}_2$ by our group⁷ and numerous others.³⁰ (One should not make rash judgments regarding the comparisons of the aforementioned density calculations and these XPS results, however, without first remembering that, other things being equal, the relative progression for XPS cross sections is $\sigma(s) > \sigma(p) \gg \pi(p)$. Thus, the observed XPS valence band results, Figure 1, may actually be in relatively closer correspondence with the band structure and molecular orbital calculations than may at first seem true.) It should be noted that the relative stabilization shifts of the O(2p) to form the latter subband is quite extensive, indicative of the strong σ -type bonding involved in silica.

2. Alumina, on the other hand, is less (bonding) stabilized than SiO_2 . In its natural hexagonal environment, Al_2O_3 tends to form only two readily discernible subbands with a very constricted gap in between. The upper subband is formed almost entirely from

(18) Holza, P.; Sauer, J.; Morgeneys, C.; Hurych, J.; Zahradnik, R. *J. Phys. Chem.* **1981**, *85*, 4061.

(19) Pantelides, S. T.; Harrison, W. A. *Phys. Rev. B* **1976**, *13*, 2667.

(20) Harrison, W. A. In *Proceedings of the International Conference on Physics of SiO_2 and Its Interactions*; Pantelides, S. T., Ed.; Pergamon: New York, 1978.

(21) Tossell, J. A. *J. Electron Spectrosc. Relat. Phenom.* **1976**, *8*, 1.

(22) Schneider, D. N.; Fowler, W. B. *Phys. Rev. Lett.* **1976**, *36*, 425.

(23) Chelikowsky, J. R.; Schlüter, M. *Phys. Rev. B* **1977**, *15*, 4020.

(24) Batra, I. P. In ref 20, p 65.

(25) Laughlin, R. B.; Joannopoulos, J. D.; Chadi, D. J. *Phys. Rev. B* **1979**, *20*, 5228.

(26) Tossell, J. A. *J. Am. Chem. Soc.* **1975**, *97*, 4840.

(27) Batra, I. P. *J. Phys. C* **1982**, *15*, 5395.

(28) Ciraci, S.; Batra, I. P. *Phys. Rev. B* **1983**, *28*, 982.

(29) Pushkarchuk, A. L.; Mardilovich, P. P.; Trokhimets, A. I.; Gagarin, S. G.; Zhidomirov, G. M. *Phys. Status Solidi B* **1985**, *129*, K181.

(30) See, for example, Thorpe, M. F.; Weaire, D. *Phys. Rev. B* **1971**, *4*, 3518.

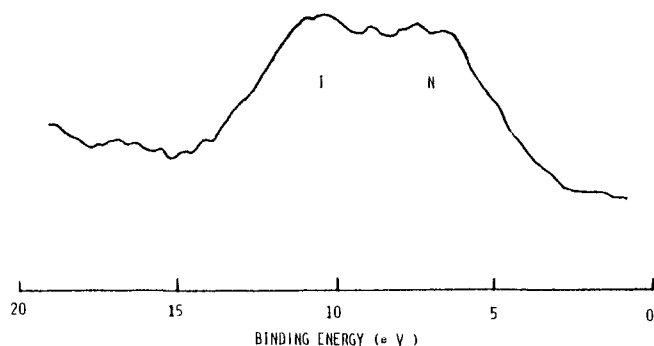


Figure 2. Representative valence band spectra for powdered α - Al_2O_3 .

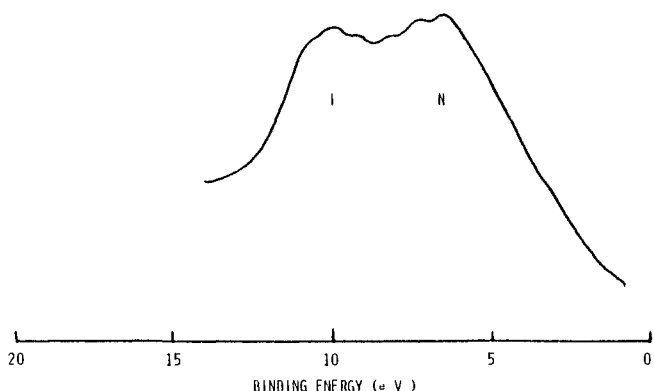


Figure 3. Representative valence band spectra for powdered γ - Al_2O_3 .

nonbonding, O(2p) orbitals, and is ~ 2 eV in width, Table II (as with the other values reported in this section, this value refers to the top of the subband). There is no apparent gap at this point, but there is a readily discernible density differentiation between the nonbonding states and the relatively close-packed bonding subband that seems to stretch for approximately 4 eV upfield from its nonbonding counterpart. The bonding states are formed from hybridized Al-O orbitals, with little Al(3s) and even less Al(3p) contribution to the density. The degree of bonding (covalent) stabilization in alumina is less than for silica. Correspondingly, the much more substantial ionicity in the former is reflected in the near total shift of the Al(3s) and Al(3p) density to the conduction band. Fairly detailed XPS valence band results for α and other aluminas have been presented by several groups,³¹ including this one.^{4,8,32} We have reproduced some of these results in Figures 2 and 3. The lack of realization of any obvious dip between the bonding and nonbonding regions for some of these measurements is not unexpected, since the obvious reduction in structural and chemical integrity experienced by the surfaces of some of the (nonpristine) materials should produce some smearing of detail. The possibility of a significant gap between the Al(3s) and Al(3p) influenced bonding regions, as suggested by SCF- $X\alpha$ calculations,²⁶ remains uncertain at the present level of experimental resolution.

As mentioned above, Tossell calculated the molecular orbital energies of the aluminum-oxygen system for aluminate in a tetrahedral environment.²⁶ In so doing, he realized the same general progression of features as Batra for hexagonal alumina,^{27,28} but Tossell also found for the former structure that all of the features are somewhat constricted in energy, toward the nonbonding region. This, as we shall see later, seems to be borne out in the experimental results, where, for example, the aluminate part of an A-type zeolite valence band is found to be pushed to

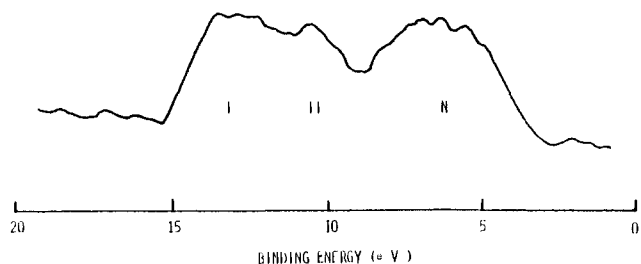


Figure 4. Typical valence band spectrum for silica gel.

the lowest possible binding energy values with significantly less bonding character than any alumina.

Summarizing these results, we present in Tables I and II an approximate rendition of where we expect the various key density points to lie, based upon theory, and realized (to some extent) in various XPS measurements.

IV. Experimental Results

A. Silica, Alumina, and Other Precursors. The first experimental problem to be considered will be to generate the valence band spectra of several of the precursor systems, notably several silicas and aluminas, and to compare the realized results with the calculations and experimental values obtained by others. In addition, we have examined other related systems, including several aluminates. The latter were included since, as indicated in several previous statements, it is our contention that *inside* the zeolite lattice the chief aluminum containing species may be *chemically* more closely associated with a metal aluminate than with aluminas.

1. Silica. A variety of ESCA studies of materials described as silica, and assumed (based upon bulk analysis) to be SiO_2 , in several structural forms, have been completed.^{7,30} There are indications that the outer (air-exposed) surfaces of these systems experience some limited degree of *surface* hydration perhaps with the formation of silanol type, Si-O-H bonds, and that this persists even when conventional steps are taken to remove *bulk* H_2O . There is particular evidence in the Si(2p) loss spectra of this hydration,⁷ but because of the resulting similarities in binding energy, there is not enough differentiation of the principal core level peaks to confirm these suppositions without substantial enhancement in both resolution and sensitivity. Controlled sputter etching and subsequent heating do seem to produce a substantially cleaner α - SiO_2 valence band spectrum, with apparent retention of structural integrity (see Figure 1).⁷ This result is representative of those also described by several other research groups.³⁰ There is no doubt that some of the undulations and peaks suggested in Figure 1 are due to the background noise representative of the resolution and sensitivity of the aforementioned ESCA system. A number of key repetitive features resulting from this particular silica are revealed, however, and these seem to match up well with those described in the calculated results in the previous section.²¹⁻²⁵ In particular, one should note the two principal subband regions separated by a deep chasm. In addition, the noticeable separation of the highest binding energy subband into at least two subsections should be considered as well as the steep nature of the leading and trailing edges and the possible structure in the low binding energy region.

It is important to pay close attention to these features, because all will be selectively altered as the structural and chemical integrity of the silica are modified. This modification does not require something as dramatic as zeolite formation; for example, one should note the slight, but critical, alterations that occur in these valence band areas for silica gel, Figure 4. In particular, one should note that the peaks and valleys for the gel seem to suffer from a kind of blunting that may, with reasonable certainty, be attributed to the corresponding reduction in structural singularity. The nature of the formation of a continuous random network (CRN) and its consequences for the glassy phase of certain oxides has been extensively considered by others.³³ These concepts

(31) See, for example: Balzavotti, A.; Bianconi, A. *Phys. Status Solidi B* **1976**, *76*, 689. Kowalczyk, S. P.; McFeeley, F. R.; Ley, L.; Gritsyna, V. T.; Shirley, D. A. *Solid State Commun.* **1977**, *23*, 161. Flodström, S. A.; Martinson, C. W. B.; Bachrach, R. Z.; Hagström, S. B. M.; Bauer, R. S. *Phys. Rev. Lett.* **1978**, *40*, 907.

(32) Barr, T. L.; Mohsenian, M.; Lishka, M. A. *J. Phys. Chem.*, to be published.

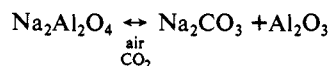
(33) Cohen, M. H.; Fritzsche, H.; Ovshinsky, S. R. *Phys. Rev. Lett.* **1969**, *22*, 1065.

obviously play a role in our analyses. Further statements about this property appear below with additional, more detailed arguments presented in several subsequent papers.³⁴ (It should be noted that, in this instance, the valence band results appear to be more revealing than the corresponding core level spectra which showed little or no difference between α -SiO₂ and silica gel.³²)

2. Alumina. The ESCA generated valence band spectra for aluminas appear to be simpler than those for SiO₂. To date, α , γ , ϵ , and catapal alumina systems have been studied with care.³² The results (see, for example, Figures 2 and 3) indicate that most of the features suggested in the aforementioned calculations are realized, particularly the two relatively small subbands separated by a chasm too narrow to record (at this resolution) except as a moderately discernible dip. No evidence is found for a high binding energy shoulder peak detected by several groups³¹ and suggested by Batra,^{27,28} as a source of ESCA revealed highly stabilized O(2p) density of states.

There is some indication in our results that the leading edge of the valence band may be somewhat higher in binding energy for α -Al₂O₃ than for the transition aluminas, but this difference may be due to the vagaries of an elusive Fermi edge. These and other possible fine details await study with an ESCA with substantially higher resolution. Certain, apparently critical, alterations of these valence bands have been detected following sputter etching and other forms of abuse. These studies play a role in the suppositions reached in the present investigation. Their details are reported in succeeding publications.^{32,35}

3. Metal Aluminates. Our studies of several commercial sodium aluminates have revealed features that seem to support our contention that the Al(2s) and Al(2p) spectra for Al₂O₄²⁻ systems are generally lower in binding energy than the corresponding peaks for most aluminas. These studies were, however, made uncertain by a persistent presence on the surface of these systems of significant amounts of Na₂CO₃ formed as a result of extensive atmospheric, room-temperature carbonation.³⁶ Unfortunately, this surface contamination cannot be successfully removed by sputter etching without also creating extensive sputter reduction of the aluminate. In order to circumvent this problem, we are attempting to generate carbonate-free Na₂Al₂O₄ surfaces, but the proper atmospheric control has not yet been achieved. We have, therefore, restricted our present analysis of the detection of peaks and bands believed to be due to Na₂Al₂O₄, in a background of Na₂CO₃ and Al₂O₃, i.e.,



B. Zeolites. 1. Introduction. In the following we describe the results obtained in examining the valence band spectra (typically long time scans over the binding energy range from 0 to 20 eV) of a variety of zeolite systems. It should be noted that certain suppositions are drawn that may in some instances seem only partially substantiated. Further verification often requires agreement with the corresponding core level results. The latter were carefully examined and previously published.^{4,6-8} Their important features are far too numerous to repeat herein. Interested readers should consult the preceding documents.

The zeolite valence band results were recorded and analyzed simultaneously from the standpoint of comparisons with other zeolites and also the aforementioned silicas and aluminas. For reasons that will become apparent later, we will divide our presentation into two sections. The first group (labeled herein as I) is made up of zeolites formed from various stackings of the sodalite (truncated cuboctahedron) and closely related cage structures, whereas the latter (group II) is devoted to chain-laced (fibrous) structural types with large [Si/Al] ratios ranging from 5 to > 100. (Figure 5, parts a-d, exhibit representative group

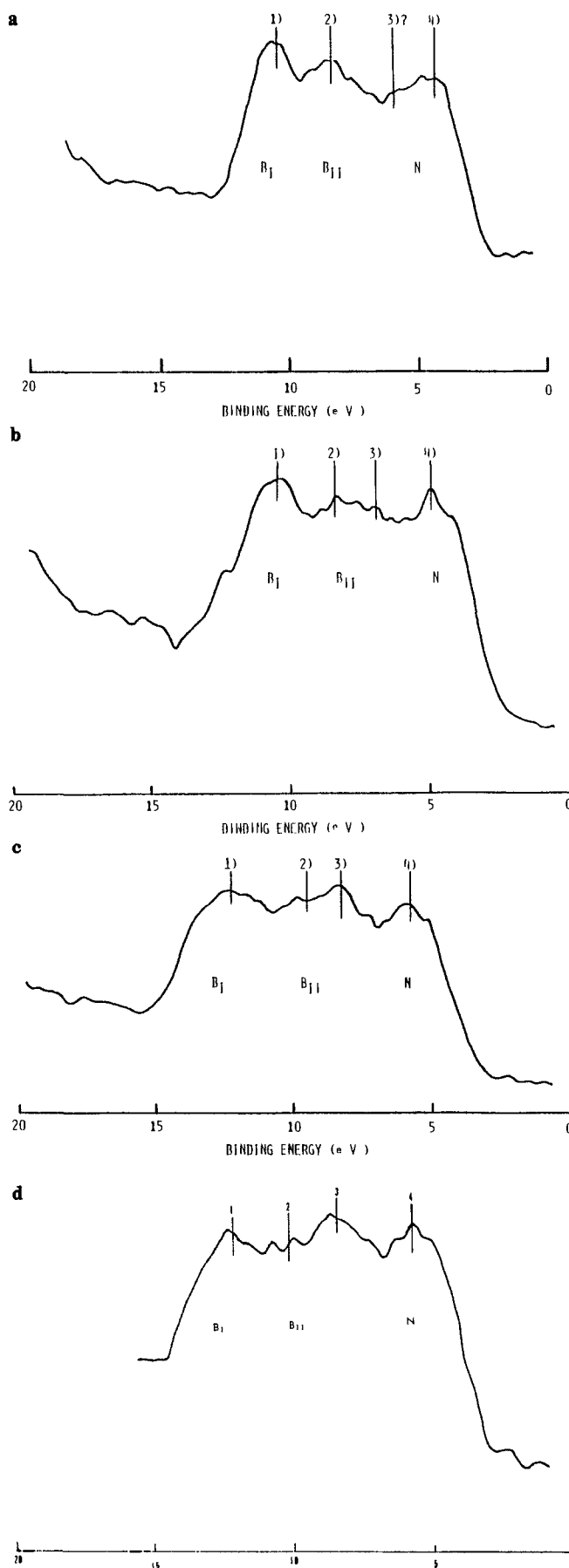


Figure 5. Representative valence band results for select (a) A, (b) X, (c) Y, and (d) L zeolites. Designations are provided for subband regions and probable peaks.

(34) Barr, T. L., to be published.

(35) Barr, T. L.; Chen, L. M.; Mohsenian, M.; Lishka, M. A. *J. Am. Chem. Soc.*, submitted for publication.

(36) Durrant, P. J.; Durrant, B. *Introduction to advanced Inorganic Chemistry*; Wiley: New York, 1962; p 811.

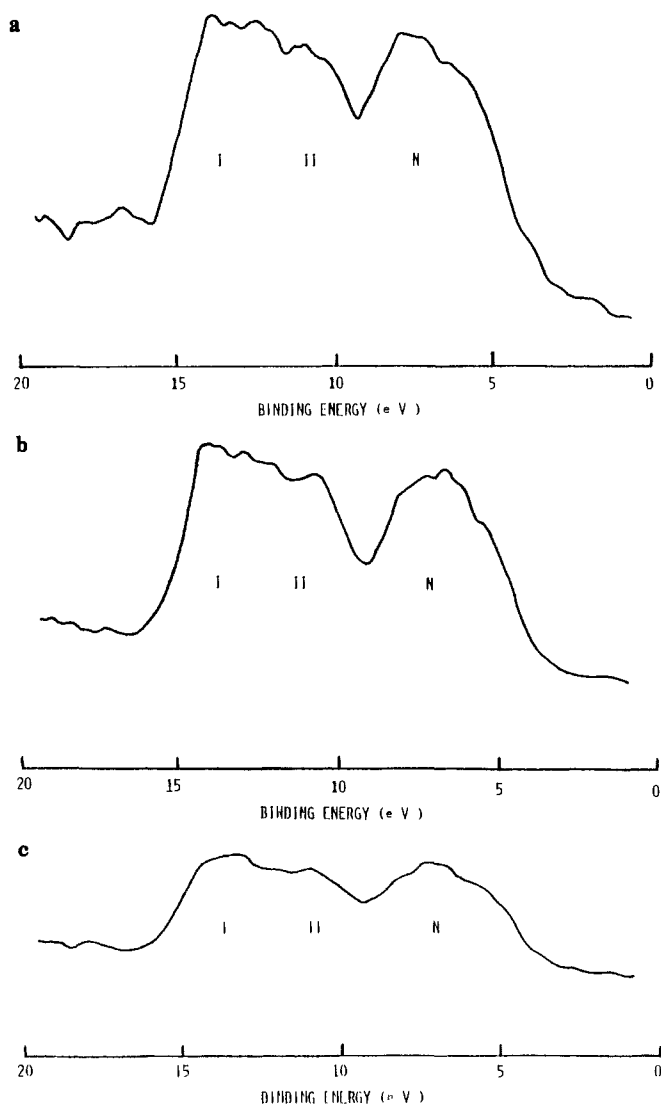


Figure 6. Representative valence band spectra for (a) mordenite, (b) ZSM-5 ([Si/Al] = 35), and (c) silicalite ([Si/Al] = 100). Subband regions are also designated.

I results, whereas Figure 6, parts a–c, are typical of group II.

Generalities. The most obvious general feature of these spectra is that many of the well-defined valence band characteristics of the silica and alumina results are truncated or altered in forming zeolites. In fact, close scrutiny reveals that the structures formed by the zeolites are definitely not just additive overlays of the “precursors”. In fact, as is seen in Tables I–III, where a number of the key factors are listed, there are many aspects that suggest substantial alterations.

2. General Precision of Valence Band Results. In the figures presented above, and the subsequent discussions, specific valence band results and simulated renditions are presented without detailed discussion of the errors involved. It should be apparent to all who have examined ESCA results that, of the numerous undulations detected in these spectra, many are due to background uncertainty and the general insensitivity of present generation ESCA's. Some reasonable criteria must therefore be applied in separating real peaks from noise.

In the present case the spectra were carefully and painstakingly produced (as described above), with extremely long scans, but, in addition, a variety of repetitions were generated to try to separate out and identify the real spectral features. The repetitions induced (i) several sequential examinations of the same material (this was used in part also to evaluate X-ray beam damage effects); (ii) examinations of different samples of the same zeolite lot; (iii) examinations of particular zeolites, e.g., NaA, from different lots and even different manufacturers that were *reputed* to be the same;

Table III. Representative Selected Sub-Band Maxima and Minima Points and Key Differences for Group 1 Zeolite Systems (in eV ± 0.25)

	Part A							
	0	1	M	2	3	N	4	5
NaY(1)	15.5	12.9	10.7	9.9	8.35	6.9	5.9	3.1
NaY(2)	14.9	12.7	11.0	10.3	8.4	6.9	5.9	2.9
NaY(3)	15.1	12.2	10.3		8.3	6.7	5.6	2.9
NaX(1)	14.0	10.5	9.0	8.15	6.9	6.0	4.7	2.0
NaX(2)	13.9	10.6	9.45	8.5	7.0	5.8	5.0	2.3
NaA(1)	13.3	10.2	9.5	8.0	5.7	6.4	4.4	1.9
NaA(2)	13.0	10.1	9.2	8.1	6.0	6.6	4.5	1.9
NaA(3)	13.2	10.5	9.0	7.8	5.5	6.0	4.5	1.9

	Part B					
	0–5	0–1	1–3	1–4	2–4	4–5
NaY(1)	12.4	2.6	4.55	7.0	4.0	2.8
NaY(2)	12.0	2.2	4.3	6.8	4.4	3.0
NaY(3)	12.2	2.9	3.9	6.6		2.7
NaX(1)	12.0	3.5		5.8		2.7
NaX(2)	11.6	3.3		5.6		2.7
NaA(1)	11.4	3.1	4.5	5.8	3.6	2.5
NaA(2)	11.1	2.9	4.1	5.6	3.8	2.6
NaA(3)	11.3	2.7	5.0	6.0	3.3	2.6

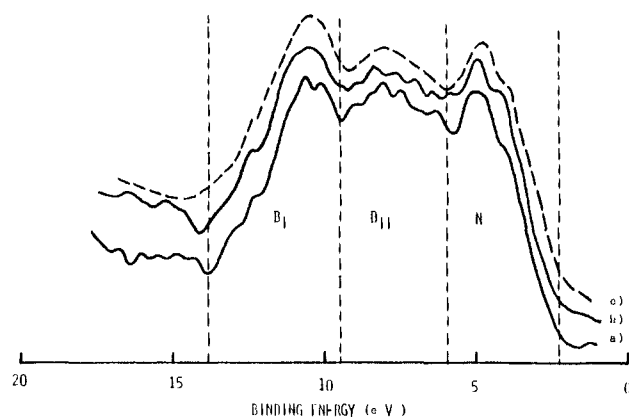


Figure 7. Overlay of selected examples (a and b) of different HP-ESCA generated NaX valence bands. A hypothetical composite (c) is also suggested. Note that the approximate scope of the subband regions is designated.

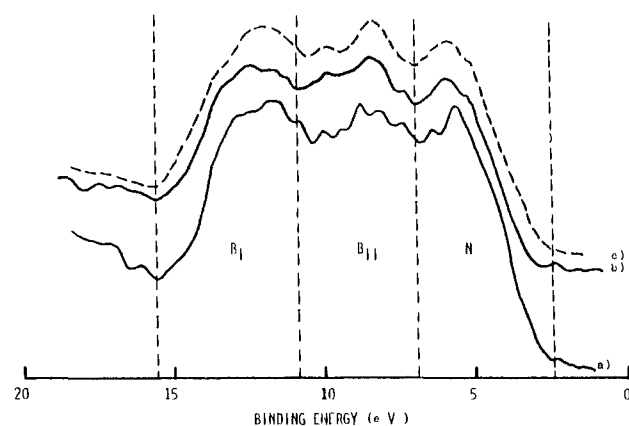


Figure 8. Overlay of selected examples (a and b) of different HP-ESCA generated NaY valence bands. A hypothetical composite (c) is also suggested. Note that the approximate scope of the subband regions is designated.

and (iv) examinations of related materials employing several different ESCA systems.

The results of these studies may be compared in a number of ways. Perhaps the most illustrative is to overlay those (of supposedly the same material) generated with the same ESCA, as is done for the two select examples, NaX and NaY, in Figures 7 and 8. Several relatively firm conclusions may be drawn from these (and related) exercises.

(i) Despite the reputed vagaries of zeolite materials preparation, two unrelated, but reputable, sources do (in these cases) seem to achieve reasonably similar spectra, suggesting closely related (*surface*) compositions.

(ii) There is strong supportive evidence here to refute any contention that ESCA is too surface sensitive to see the "real" zeolite, instead focusing on surface degradation byproducts. If that contention were true, one should not find numerous examples of materials from dramatically different histories that produce the same spectrum, with such repetition of detail. In addition, the lack of additivity of the precursor spectra referred to above also supports this refutation. In fact, as we shall see, the spectra detected yield a consistent pattern based on the criteria that the ESCA is detecting sufficient parts of the unaltered zeolite lattice to make meaningful identifications.

(iii) Occasionally, small differences were found in the binding energies determined for the same species in different samples. Thus, during attempts to overlay the valence band spectra of supposedly identical material, it was occasionally necessary to make small energy shifts to achieve good overlap. In every case, these shifts produced complete overlaps of all peaks and bands, suggesting that the problem was generally due to inaccurate energy scales (uncoupled Fermi edges), although one should not preclude some shifts due to a variety of possible trap states, and other chemical and physical causes. The general tabulated and presented results have, where necessary, been selectively shifted to alleviate any scale problems.

(iv) Sufficient precision and repetition is suggested in these overlays to produce a collective, representative spectrum for each material (see, for example, Figures 7c and 8c). Only the most certain features are reproduced in these representations, and we have purposefully assumed a relatively poor degree of resolution in mimicking their size and shape. Obviously, many subtleties are omitted in this "broad brush" picture, but we wanted to restrict our subsequent discussions to only those parts that we feel assured are reasonable and important components of true (zeolite induced) subband features. Further, more refined, analysis awaits a study employing ultrahigh resolution ESCA. This will be performed in the near future.

(v) One should note that, for the reasons enumerated above, the representative selections of the results achieved with ESCA systems other than the HP, e.g., in Figures 9 and 10, generally do not exhibit the same degree of resolution, but close comparison does show that *all of the major features* detected by the HP are found for a particular zeolite using the other systems.

3. The "Tetrahedral Aluminate into Silica" Concept. One of the difficulties with the previously described ESCA core level study of zeolite systems concerned the unique nature of the shifts realized. Thus, we found that when the type of zeolite being examined by ESCA was changed, all of the core level binding energies shifted, but sometimes *all of the (elemental) peaks* seemed to shift in the same direction, rather than the more common result of some peaks shifting to higher binding energy (indicative of enhanced oxidation), while others would simultaneously shift to lower (reduced) binding energies.

In the case of the zeolites in question, the explanation for the single shift direction seems to be based upon the difference in ESCA behavior of the basic zeolitic "chemical ingredients", silica and sodium aluminate, rather than the elements. Thus, the binding energies of the oxygen, as well as the silicon, are relatively large for SiO₂, particularly compared to those for NaAlO₂. Tetrahedral substitution of a small amount of the latter into a particularly structured (zeolite) lattice, largely of the former, causes a substantial upfield adjustment of the aluminate (as it accommodates

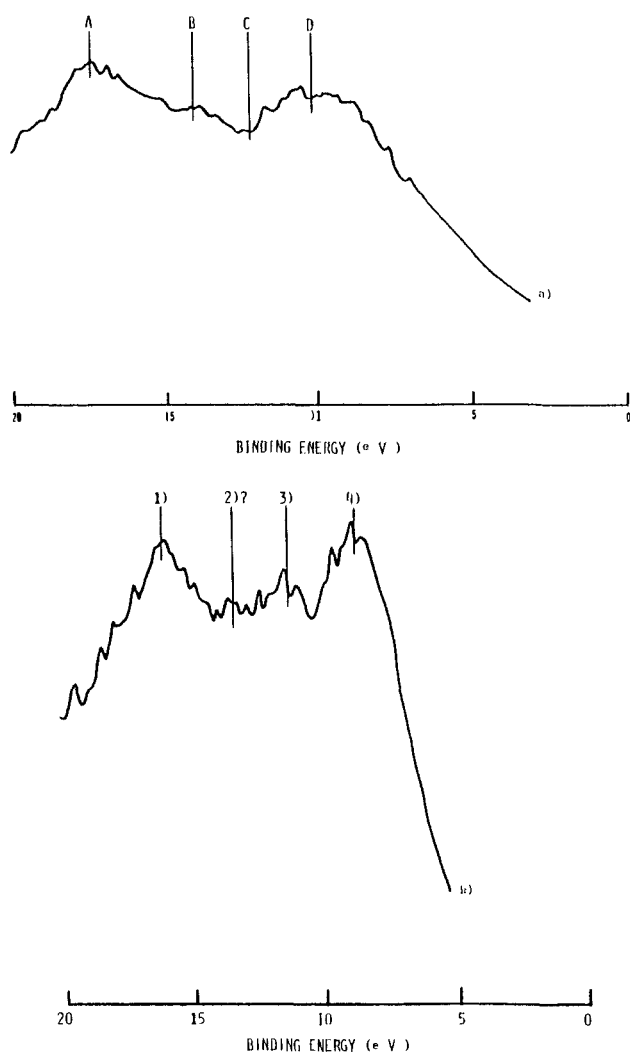


Figure 9. Valence band spectra for selected zeolites, (a) ZSM-5 and (b) NaY, produced using a Leybold-Heraeus ESCA with shorter scan times and no data treatment. Note crude match with HP-ESCA results.

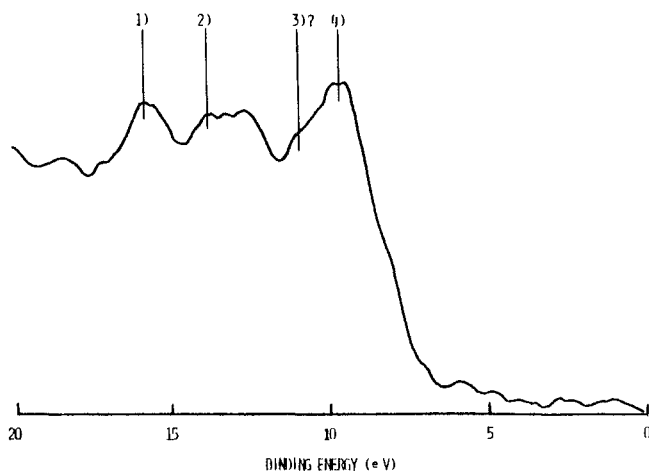


Figure 10. Valence band spectra for NaA achieved with long time scan using PHI 5300 ESCA. Note similarity to Figure 5a.

to the tetrahedral, silica dominated quantum fields), and a corresponding slight reduction in binding energy of the SiO₂. As more aluminate is introduced into the zeolite, the dominance of the silica is broken and it begins to shift more dramatically downfield, whereas the aluminates are correspondingly less affected. This process continues as more and more aluminate is "forced" into the tetrahedrally oriented zeolite lattice until it reaches the (one-to-one) limit at NaA, where the dominant characterization

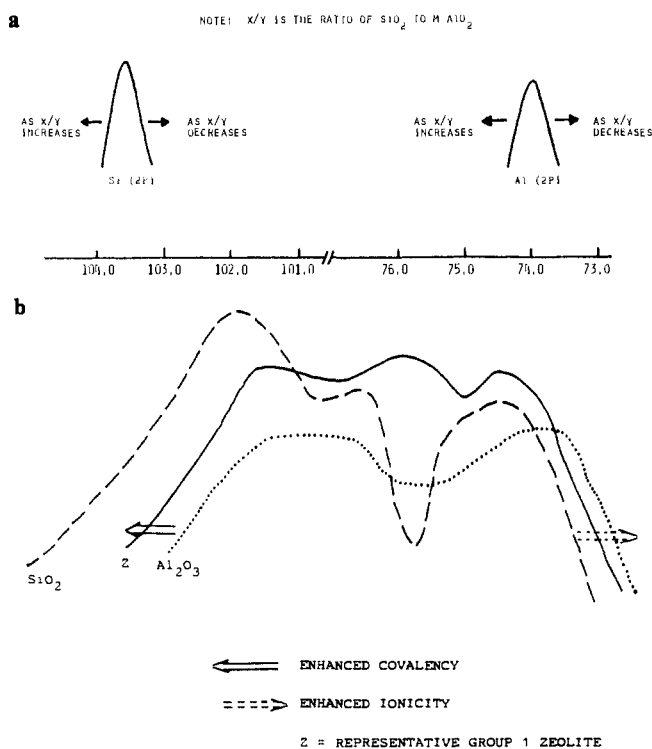


Figure 11. Figurative rendition of "chemical" shifts realized by concept that zeolite formation results from the substitution of MAlO_2 into SiO_2 : (a) core levels, (b) valence bands.

is essentially reversed. In this latter case, the NaAlO_2 part of NaA exhibits ESCA results almost like those of a pure aluminate. (It should be noted that the Na, Al, and O binding energies of NaA are less than those for a typical alumina.) Thus, in a sense, just as we might expect, in these lattices the aluminate system is somewhat electron proficient and is thus able to donate electrons to the relatively positive silica units.

The generality of this postulation is expressed somewhat loosely, in a pictorial manner, in Figure 11a. (Note that we should also observe that substitution of multivalent cations for Na^+ in many of these systems acts (perhaps through the dispersion of charge) to independently modify these fields and shift the resulting photoelectron peaks.)^{4,7}

There may be a direct correspondence between our observed chemical shifts and certain quantum cluster calculations of the $(\text{OH})_3\text{Si-O-Al}(\text{OH})_3$ unit by Derouane and Fripiat.^{15b} Thus, they find that in this cluster, Si is more electropositive than Al and the $\text{Si}(\text{OH})$ units are less negative than the $\text{Al}(\text{OH})$ units; all of this seems consistent with the group influenced binding energy shifts suggested in the present study.

Of particular importance in the present discussion is the fact (as presented below) that the shifting pattern alluded to in Figure 11a is also borne out in the behavior of the corresponding valence band (VB) structures. Thus, it would appear that all of the factors that have been suggested to reflect upon the status of a particular zeolite become involved. For example, in Tables I and III we find (i) the VB leading edge of NaA has (of all the systems examined) the lowest binding energy, whereas silicalite has the largest; (ii) the bandwidths at half-maximum follow a similar progression from smallest (NaA) to broadest (silicalite). (iii) In addition, the relative contribution of oxygen to that part of the valence band that seems to be bonding stabilized by silicon increases in the same manner (see below). (iv) Similar statements may be made about the relative contributions of aluminate species, their binding energy positions, and their band shape relative to those for various aluminas. Definitive realization of these results still awaits examination with an ultrahigh resolution ESCA, and, therefore, only a few preliminary suppositions have been reached (see below). The valence band results to date do suggest, however, that zeolites with a $[\text{Si}/\text{Al}]$ ratio of 5 or greater are composed of slightly perturbed silica with aluminate doped into it, whereas NaA is

essentially the opposite. Further aspects of these arguments and their relationship to chemistry and structure, and also the so-called persistence/agglomeration concept,³⁷ will be discussed later. (v) It should also be noted that substitution of multivalent cations for Na^+ modifies the valence bands of these zeolites in reproducible ways. A more detailed account of the latter results and our speculations regarding them will be presented in a subsequent publication.³⁵

Thus, the patterns of behavior detected for the various zeolite valence bands under present scrutiny exhibit substantial support of the concepts embodied in Figure 11a. This concept, in which a zeolite is loosely construed as a quasi-substitutional solution, of two precursors whose electronic components extensively interact with one another, will be reconsidered below in a slightly different context. Figure 11b is presented as a suggestive precursor to that context, in which substitution of various amounts of aluminate into silica to form a zeolite causes significant covalency/ionicity shifts in both precursors, while forming a new bonding environment.

4. General Features of Group I Zeolites. The following features would appear to be reproducible parts of the valence bands of the zeolites designated as members of group I; see, for example, Figures 5, 7, and 8 and Table III.

(i) There seem to be three major subband regions (hereafter labeled as B_1 , B_{11} , and N, respectively) separated in most instances by modest depressions.

(ii) There appears to be some fairly extensive mixing and shifting, particularly in the middle subband region, B_{11} , depending upon the type of zeolite being examined. In the case of NaA , there is primarily one sizable subpeak in this middle region (labeled as peak 2 in Figure 5). In the case of NaX , there appears to be a broad subpeak roughly in the middle of the subband. Parts of this peak are definitely shifted to a lower binding energy than the aforementioned peak in NaA . In the case of NaX , the peak is so broad that it may be a multiple peak structure. In the case of NaY , there is a further shifting in structure, such that a new peak (labeled as number 3 in Figure 5c) definitely occurs at a much lower binding energy than that of peak 2 for NaA . In addition, a smaller, separate peak is suggested for some NaY samples near the position of peak 2 found for NaA .

(iii) In the case of these group I type valence bands, the upward slope of the leading edge, as well as the downward slope of the trailing edge, is far more gradual than that displayed by SiO_2 , being instead more like the various alumina valence bands examined.

(iv) Peak 1, in the first subband, B_1 , is always much smaller than the related bonding orbital section of a SiO_2 valence band. This peak seems to vary in size, sometimes being quite small (singular-discrete) and at other times moderately broad.

(v) The peaks involved with the third subband region (N) also seem to vary in size. In this case, they seem to achieve their best definition for NaA where it is possible that two peaks may be involved: 3' on the inside shoulder and 4, the principal protrusion. In the case of NaX and NaY the present resolution limits the definition, and only one peak, 4, has been identified.

(vi) The valence band of the NaL zeolite systems would appear to resemble very closely those produced by the NaY systems.

(vii) The falloff in detected density between the identified peaks is quite small, suggesting that secondary (and even primary) points of orbital density may be occurring in these areas, as well as near the detected peaks.

5. Group II Zeolites: Mordenite, ZSM-5, and Silicalite: Comparisons with Previous Studies. In addition to the A, faujasite, and L systems, it is important to consider the valence band spectra of zeolites with larger $[\text{Si}/\text{Al}]$ ratios. In this regard, we shall find it interesting to examine representative mordenite, ZSM-5, and silicalite systems. For reasons that will become more apparent later, the results will also be explicitly compared to those bands obtained during examinations of the previously mentioned zeolites with smaller $[\text{Si}/\text{Al}]$.

(37) Onodera, Y.; Toyozawa, Y. *J. Phys. Soc. Jpn.* **1968**, *24*, 341.

Examples of the realized results for group II zeolites are displayed in Figure 6, a–c.

It should be noted that although the mordenite species studied contained (like the previous zeolites) almost exclusively the sodium cation, Na^+ , this was not the case for the ZSM-5 and silicalite materials (both containing substantial percentages of organoamine cations). This apparent deviation from the previously established pattern was necessitated by the peculiarities in the preparation and stability of the pentasil systems.³⁸ Based upon our results with many zeolites following cation exchange, there is little doubt that the use of cation substitutes for Na^+ slightly alters the core level⁷ and valence band ESCA spectrum for that zeolite lattice (see Zeo VII³⁵ for the details behind this statement). However, it is also apparent that the general results described in the following analyses will be only slightly perturbed by the present substitution of an organic, monovalent cation.

In addition to the aforementioned deviation, it should be noted that we have included our best guess as to the average results (at this level of resolution), while not including any overlays. Repetitive overlays may be made for these large [Si/Al] ratio zeolites, but one must be very careful at this point, since commercial preparation of those systems has been shown to be extremely susceptible to relatively large surface concentrations of alumina and aluminate type byproducts.⁸ When detected, these byproducts must, of course, be removed to provide a reasonable set of core and valence band results for the (pure) zeolites. The stagewise development of the latter cleaning process is, in itself, an interesting and important process (as is dramatically described in Zeo VIII⁹). The results presented in Figure 6, a–c, are, therefore, the valence band spectra for the resulting, relatively clean, systems.

Several general features are immediately obvious when one compares the valence bands of these large [Si/Al] zeolites of group II with that for silica, those produced by the previously studied zeolites with smaller [Si/Al], Group I, and themselves. These generalities are as follows.

(i) The valence bands of the members of group II are all quite similar.

(ii) These valence bands closely resemble that for silica.

(iii) The valence bands for group II are substantially different from those of the members of Group I.

(iv) Valence bands for group II thus all exhibit a broad subband at relatively large binding energy that often seems to be divided into several discernible peaks. This subband is then separated from the other major subbands by a relatively deep chasm, where the detected density of states must drop precipitously. The lower binding energy band also seems to exhibit a similar roughly repetitive pattern, although the subpeaks that may be detected (and are often comparable to those reported by others^{25,30}) do not seem to follow any explicable pattern. Perhaps the most interesting feature is that all systems from silica to mordenite seem to exhibit the same basic pattern, with only slight, but progressive, evidence of lack of silica-like resolution as the [Si/Al] ratio decreases from 100 (silicalite) to 5 (mordenite). *When one progresses farther to L (Si/Al = 3) and Y (Si/Al = 2.5) zeolites, there is a dramatic change in the pattern of the valence band structure that, in turn, seems to persist down to NaA (Si/Al = 1) (see the previous section).* The latter feature is, in fact, the principal basis for the group I–group II distinction.

6. Detailed Features of the Valence Bands of Group I and II Zeolites. a. Numerical Results. Close scrutiny reveals that there are a number of additional features that may distinguish the bands in group II from those in group I and also from each other. In order to realize the consequences of these fine points, we will first consider some numerical relationships that may be generated by labeling some of the key points in each (representative) band and noting the resulting binding energies. Some of those values are listed in Tables I–III. These values are, of course, susceptible to the previously described uncertainties in removal of charging and establishment of a truly universal Fermi edge.^{4,7,14} We will,

therefore, concentrate most of our subsequent consideration on the *differences* between some of the points that are listed in Tables I–III. Because of the rather substantial margin of error also associated with these results, we are inclined, at this stage, to place significance on the relative values and trends, rather than the absolute numbers. The following relationships seem to be most pertinent.

(i) It should be noted that the *total* bandwidth (0–5), as detected by the ESCA, for the examples described, is slightly broader for silica (~ 12 eV) than alumina (~ 10.5 eV). These values are within the scope of some of the calculated values that suggest ~ 12 eV for both.²⁸ Consistent with the present results, there are also indications in these calculations that the valence band for silica may be somewhat broader than that for the aluminate.²⁷

(ii) There is some suggestion that the *total* bandwidth for the zeolites with large [Si/Al] ratios may be somewhat broader than that for silica alone. This is perhaps suggestive of the presence of a nonbonding aluminate dominated tail that may occur on the leading edge (low binding energy side) of the zeolites.

(iii) The energy spread of the principal subband peaks with the largest separation (1–4) (or A–E for silicas, aluminas, and Group II zeolites) is, as expected, substantially narrower than the total bandwidth (0–5). In this case the spread of the most bonding peak (1 or A) from the most nonbonding (4 or E) is much larger for the silica dominated systems than those relatively rich in alumina-like species. *In fact, there appears to be a progressive drop in this width from ~ 8 –9 eV to 4–5 eV as one reduces the percent of silicon from 100 (silica) to 0 (alumina).* This suggests that there are substantial “wing” portions on either side of the valence band density of states of alumina and aluminate dominated systems (Figures 2 and 3) that interact, but do so weakly, with the XPS photons, and that the same is not true for the density of states of silica where the drop is quite precipitous (Figure 1). That this should occur on the leading edge (low binding energy) side is not surprising in view of the greater ionicity of alumina, and the corresponding enhancement of the relative importance of the nonbonding electron character in its total O(2p) electron density. (Note that the relative general cross section of valence state electron density (Δ) in the XPS experiment seems to be $\Delta(\sigma_s) > \Delta(\sigma_p) \gg \Delta(\pi_p)$.) On the high binding energy side of the alumina valence band, the gradual falloff (compared to silica) from the XPS detected peak may be attributed to the relatively more diffuse (ionic) contribution of Al(3s) orbital density compared to Si(3s),²⁴ or perhaps to the presence (under these conditions) of substantially more localized Cohen, Fritzsche, and Ovshinsky^{33,34} tail states for alumina compared to silica. The XPS detected spread in the subband peaks strongly suggests that there is a greater (bonding) stabilization energy being exerted in silica (compared to alumina) with a much broader separation between the bonding and nonbonding density (i.e., the relatively large chasm for silica at C). Thus, the spread across the *top* of the higher binding energy (bonding) subband for silica is substantially broader than for alumina, whereas, although the same order occurs for the lower binding energy (nonbonding) subband, it is much less pronounced. Because of the more extensive mixing of subband peaks in the case of the zeolites, the latter feature cannot be directly followed for these materials; however, as shall be pointed out below, it seems to play a role in the realized results.

(iv) In the case of the group I zeolites under study, one should note that we have identified four (4) major subband peaks (labeled as 1, 2, 3, and 4). Some version of these peaks is suggested to occur for all of the group I systems. Examination of the individual spectra, e.g., Figure 5, a–c, suggests that if this contention of only four peaks is true, then they must also exhibit variations in relative size and shifts in their position. Obviously, since a principal variant between these systems is the [Si/Al] ratio, one can assume that these peaks, and their size and position, in some way, are reflections of the relative size of that ratio. In a similar fashion, the formation of different zeolite structures also plays a role. In the Discussion below, we will put together these and other experimental observations in an attempt to speculate upon the origins of these various subband features.

(38) Derouane, E. G.; Detremmerie, S.; Gabelica, Z.; Blom, N. *Appl. Catal.* **1981**, *1*, 201.

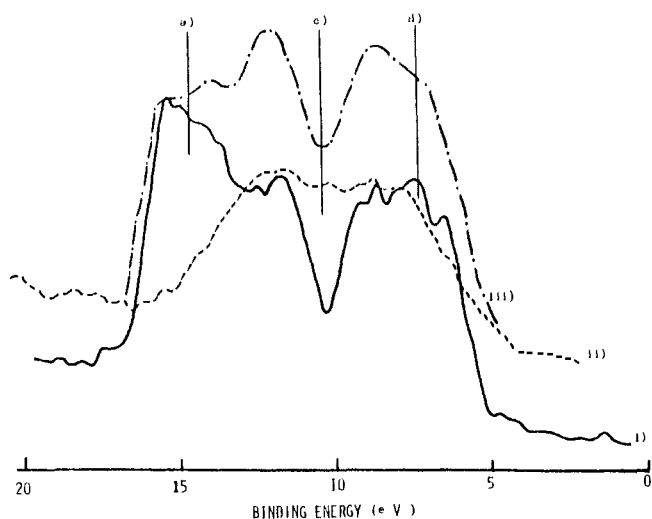


Figure 12. Rough overlay of selective (1/1) mixture based upon experimental results in Figures 1 and 2: (i) α -SiO₂, (ii) α -Al₂O₃, and (iii) the "nonchemical" composite.

(v) In a related manner, one may analyze the subband features of the group II zeolites. In these cases, however, the features are sufficiently similar to those for silica (α -quartz and silica gel) to permit one to develop a relatively consistent, "broad brush" picture by arguing that the group II species appear to the ESCA to be (unlike the group I zeolites) silica with increasing amounts of aluminate perturbation (silicalite \rightarrow mordenite). Thus, we find for the group II systems increasing evidence of finite electron density outside the range for silica, i.e., (0-A) and particularly (E-5). In addition, the subband peak spread narrows, and the position of the bonding-nonbonding chasm shifts. These are all features that suggest the presence of a perturbing density of states in the middle of the silica band. Arguments will be presented below speculating as to how that perturbation is created by the aforementioned aluminate, selectively located *inside* the zeolite structural unit. One must be wary, however, of the possible presence of other alumina/aluminate nonzeolite byproducts, which we have already demonstrated may be a relatively persistent residue found in freshly prepared versions of these zeolites.⁸ Efforts were employed, however, to remove these byproducts before generating the present results, and all indications suggest reasonable success.^{8,9} A detailed ESCA analysis of a typical purification process is presented in a separate publication in this series, Zeo VIII.⁹

b. Comparative Stacking of Valence Bands of Different Zeolites.

In addition to comparisons of numerical values, it is informative to consider the features of these valence bands that may be realized when experimental bands for different systems are overlaid. Unlike the previous overlays of valence band spectra of purportedly the same species, the present procedure is made difficult by the obvious shifts that move the entire spectrum (see ref 7). These shifts have been previously established to be real,⁸ yet it is also apparent that many of the subband features realized in the different zeolite valence bands are, in fact, the same feature, merely displaced by these shifts. Therefore, examples are needed that present both shifted and unshifted overlays.

Perhaps the most important unshifted result can be obtained by overlaying typical results for α -quartz and α -Al₂O₃. This is done in Figure 12 (where we have assumed $C_1/C_2 = 1$, while simultaneously recognizing some differences in cross sections). The resulting manifold is interesting in that several major subsections seem to occur, with a few potential peaks in each section. If we compare this overlay with the features detected for the zeolite with $C_1/C_2 \approx 1$, NaA, Figure 5a, we see immediately that there are a variety of obvious differences. First, the manifold silica-alumina overlay band is much broader than that for any zeolite system. Second, the NaA system produces the narrowest valence band of any zeolite system, far narrower than the aforementioned overlay. In fact, it is apparent from this exercise that two features may be simultaneously occurring during zeolite formation: (i)

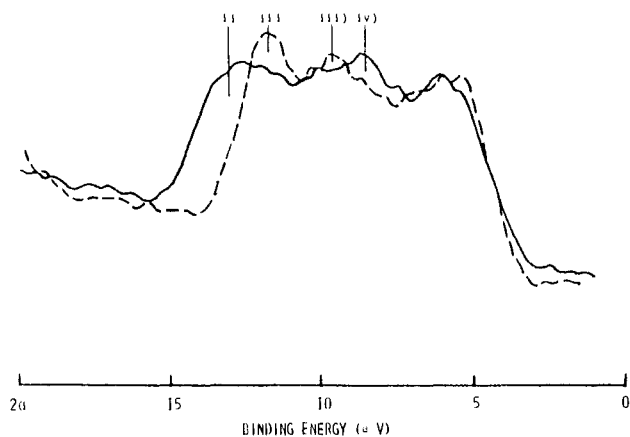


Figure 13. Comparative stacking of selected valence band spectra for (---)NaA and (—)NaY: (i) enhanced silicon (3s?) bonding region in NaY, (ii) shifted, narrow silicon bonding region in NaA, (iii) "excess" aluminum bonding region in NaA, and (iv) silicon influenced nonbonding region in NaY.

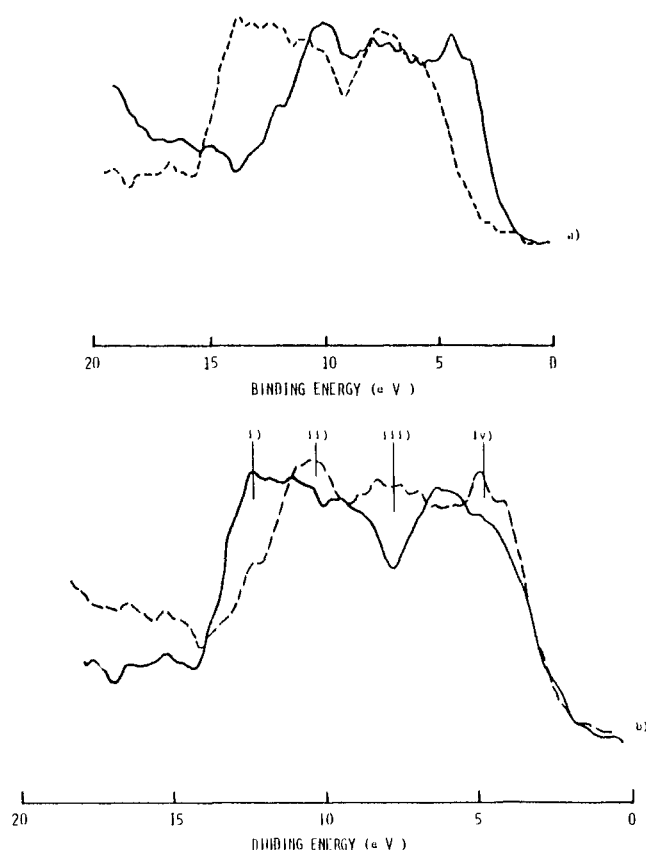


Figure 14. Comparative stacking of select valence band spectra for NaX (—) and mordenite (---): (a) unshifted overlay; (b) shifted overlay to match leading edges: (i) enhanced silicon (Si(3s)?) bonding region in mordenite, (ii) condensed silicon bonding region in NaX, (iii) mordenite chasm filled in NaX band by aluminum bonding, (iv) nonbonding (O(2p)) region due to enhanced presence of aluminum in NaX.

as previously outlined, mixing of SiO₂ with MAIO₂ seems to shift the silica part down in binding energy, while simultaneously shifting the aluminate part up, while (ii) some of the subfeatures of the two separate band structures (silica and aluminate) appear to be dramatically curtailed (or perhaps even entirely removed!). The latter curtailment seems to be particularly realized by that part of the silica valence band spectrum produced in the bonding region stabilized by Si(3s) electrons (see designation I in Figure 1). In view of these conditions, we will construct a few representative zeolite overlays with selective shifts of one or both of the valence bands in order to maximize the comparative information.

Several overlays of the valence band spectra of zeolite systems are presented in Figures 13 and 14.

Figure 13 was produced by purposefully matching the leading edge (low binding energy side) of the NaA and NaY valence bands. This was accomplished by noting that the structures of the subbands seem to be growing in width from right to left. It also appears that the last subband (lowest in energy), N, may be caused for these two systems by relatively similar nonbonding orbitals. Assuming this to be logical, one finds that the rest of the subband features all shift to unique values for the two matrices. In particular, as noted above, there may be a compatible subband peak (4), whereas the peaks in the center subband region exhibit unique distributions as exhibited in Figure 13. Perhaps the largest variation, however, is the apparent contraction of the first (highest binding energy), B₁, subband for NaA compared to NaY. Based upon comparisons with the SiO₂ precursor results, one can reasonably assume that this subband is formed almost exclusively from silicon stabilized (bonding) O(2p) orbitals. Yet, it is apparent that the XPS detected density of states for this expansive region in the case of SiO₂ (see Figure 1) has been extensively collapsed for NaA into a rather singular peak in the region with the largest possible binding energy. The contraction of the detected density in the case of NaY is much less than NaA, suggesting some kind of progressive effect due to the changes in the [Si/Al] ratio.

The latter effect appears to have some continuity when extended to larger [Si/Al] ratios, Figure 14. In this case, however, at first (Figure 14a), we have not shifted the spectra to create any forced overlay, instead relying on the shifts detected from the (supposedly) correct universal Fermi edge (see section 2 and ref 8 and 15). Now we see that the transition from NaX to mordenite ([Si]/[Al] changes from 1.2 to 5) occurs with some type of dramatic change in total valence band structure, as well as the shifting effects. In fact, the shifts in XPS detected density with an increase in the [Si/Al] ratio may be approximately realized by noting the directions of the flowing arrows in Figure 11b. Details of the internal shifts are amplified in a forced overlay in Figure 14b. In particular, one should note the growth of both the central chasm and the substantial Si-induced bonding stabilization density in mordenite relative to NaX.

It should be noted that the previously described shift to align the leading edges of these valence bands is not nearly as capricious as it may first seem. In fact, it will be later argued in detail that the removal of the variable chemical shifts of the aforementioned nonbonding O(2p) electrons for these oxides reveals the *true* bonding shift induced by differences in covalency and ionicity.³⁹

V. Discussion

A. Valence Bands of the Group I Zeolites: Compositional Considerations. In the previous section, the valence bands for the zeolites from A to L were found to be subdivided into three primary subband regions, labeled herein as B₁, B₁₁, and N. The two end regions, B₁ and N, do not appear to be very similar to the subband regions documented for silicas or aluminates, but one can still employ the details of the latter as suggestive models in hypothetical arguments of the type of orbital development in B₁ and N. Thus, basic logic would require that the region B₁ is dominated by contributions from bonding-type orbitals, whereas N is formed primarily from nonbonding-type orbitals. Except to say that the principal orbital contribution to all of these densities is, no doubt, O(2p), one cannot make many *absolute* statements about these subbands without, at least, the support of fairly detailed band structure (or molecular orbital) calculations. (One should keep in mind, for example, that there is a significant possibility of oversimplification in trying to identify the sources of modest peaks in a relatively large background density. Thus, the detected peaks may actually represent the points of maximum overlap of several orbital densities whose true (hidden) peak maxima may be at distinctly different points in energy space.) By putting together all of the facts, however, it is possible (in our opinion) to develop a fairly reasonable depiction of the major features of these subbands.

a. B₁. This label is employed to designate the subband region with the most substantially stabilized bonding orbitals. In addition, for B₁:

(i) Based upon the binding energies realized by this subband, we suggest that it is formed primarily from O(2p) σ bonding orbitals primarily stabilized by silicon (3s and 3p) orbitals.

(ii) In view of the fact that the aluminate system seems to produce a shift to lower binding energy compared to alumina, we do not anticipate that there is any appreciable Al(3s or 3p) stabilization of O(2p) in this region for any of the zeolites, particularly because the subband seems to shift to higher binding energies in concert with the shifts of the Si rather than the Al core level peaks.

(iii) The relative contribution of the silicon orbitals themselves to the density of states of this subband should be, for all group I zeolites, significantly reduced compared to that for SiO₂. Thus, the general shift to lower binding energy suggests a somewhat enhanced ionicity of the silicon-oxygen bond, particularly for the NaA system.

(iv) This general shift does support the concept of a significant overall reduction in photoelectron intensity, but it does not account for the *dramatic contraction of the breadth of this silicon stabilized region for these zeolites compared to that for silica* (or, for that matter compared to all the zeolites of group II). This contraction of subband B₁ was shown to be continuous from L to A. Part of this reduction may be accounted for by assuming that some of the Si(3p) stabilized O(2p) has been shifted into the (yet to be discussed) B₁₁ region, but a number of factors, including the size of the shifts involved and the relative size and number of peaks in B₁₁ and N, suggest that this may be the principal reason for the shrinkage. We are, therefore, forced also to accept the concept of a significant contraction in the total breadth (in energy) of the silicon stabilization of these orbitals. In fact, overlays of the type described in the previous section suggest that most of the aforementioned density in NaA has been squeezed into a region comparable to that stabilized primarily by Si(3p) in silica. It also appears that the width of B₁ does increase somewhat with the [Si/Al] ratio. This would seem to suggest that most of the large covalent stabilization realized in silica by the hybridization of the silicon 3s²3p² electrons, coupled with O(2p), is substantially repressed in these systems, particularly for NaA. At the same time, there is increasing π -type nonbonding character for the O(2p) states in N for these zeolites. Therefore, it is tempting to attribute the contraction of the B₁ subband to a reduced tendency of Si(3s) to participate in the bonding stabilization of O(2p), particularly in NaA and NaX. If this is true, one must still account for the density of Si(3s) electrons. At least two points need to be considered. (a) Any creation of nonbonding Si(3s) electrons should result in an appropriate shift of some of the previously stabilized O(2p) density. This may also shift some of the Si(3s) density into the B₁₁ or N region. (b) An alternate, and perhaps more appropriate, explanation suggests that the silicon-oxygen bond is made increasingly ionic by the substitution of aluminate. If this is true, it would tend to destabilize the normal tetrahedral bonding, shifting some of the O(2p) density into the nonbonding region, while simultaneously enhancing the contribution of Si(3s) states in the conduction band.

(v) All of this is consistent with the concept that extensive aluminate substitution into the silica tetrahedral lattice dramatically perturbs that lattice, until in the one-to-one concentration range, around NaA, the zeolite system is more appropriately described as silica substituted into tetrahedral aluminate, and the silicon valence orbital behavior essentially mimics that of the aluminum.

(vi) It should also be noted that the reduction in the width of the silicon stabilized (bonding) density is consistent with the application of the Lowenstein rule. Thus, as has been demonstrated by Batra^{24,28} and Tossell,²⁶ the width of this bonding section is, in fact, a function of the degree of *chemical* continuance of any Si-O-Si-O-Si- chain (or cage). Interjection of Al for Si in these units should definitely reduce the extent of the silicon stabilization. Lowenstein-forced alternation of Si and Al, as in NaA, may almost obliterate that stabilization. (The implications

(39) Barr, T. L., to be published.

of these features will be discussed further below.)

b. B₁₁. This subband region in the middle of our group I zeolites is dominated by one or more peaks that may, in fact, shift with zeolite type. Further:

(i) If our assumptions about B₁ are true, then B₁₁ should contain significant contributions due to the bonding stabilization created by the aluminate part of the group I zeolites. (ii) This region also will contain any silicon stabilized bonding contributions that are not located in B₁. (iii) In succeeding arguments we will attempt to show that this region also contains significant density of states from O(2p) nonbonding orbitals associated with certain aspects of the silica part of the various zeolite lattices. (iv) Very little can be said with certainty about the identity of the individual peaks detected in this subband region. We have previously detected two (labeled as 2 and 3) in NaY and NaA while suggesting that the rather broad peak detected in the middle of B₁₁ for NaX may be multifaceted, perhaps a mixture of 2 and 3 (see Figure 5b and Table III). Based upon the following three factors, (a) relative peak size and change of size, (b) shifting in binding energy, and, perhaps most important, (c) changes in relative peak size during the selective sputter etching of these systems (the details of this useful examination are presented in Zeo VII³²), we have made the following somewhat speculative assignments for these two peaks. Peak 2 is formed *predominantly* from O(2p) orbitals that have been bonding stabilized by Al(3s) and Al(3p) orbitals. This supposition is based upon the relative size of 2 in NaA compared to NaY; it is ~4-eV splitting from peak 4 (to be discussed later) and the favored retention of peak 2 following sputtering.³⁵ (Note that a relative sputter removal order of O ~ Si > Al has been detected.^{7,32,35})

Peak 3, on the other hand, is suggested to result primarily from O(2p) nonbonding orbitals associated with the previously defined bonding part of the Si-O system. This judgment is based on the splitting of 3 from peak 1, comparisons with the bonding/nonbonding splittings for silica (i.e., note the B-D and B-E values in Table I), and similar relative size and sputtering arguments as employed above for peak 2. (Note the size of 3 for NaY!)

In the case of NaX, the broad peak seems to reside somewhere in between the positions for peaks 2 and 3 in NaA and NaY. If one suggests a splitting of ~4 to 5 eV between bonding and nonbonding peaks, and also employs the relative peak size vs. [Si/Al] ratio arguments, then it seems reasonable to assume that this broad (NaX) peak is an agglomeration of previous peak 2 (Al(3s) and -(3p) stabilized (bonding) O(2p) on its high binding energy side) and peak 3 (O(2p) nonbonding orbital density resulting from the silica-like part of the NaX system on its lower binding energy side). These features are suggested in Figures 5b, 7, and 14.

c. N. This subband region is composed entirely of nonbonding O(2p) orbitals. Because of the nature of the binding energy involved, the splitting from the aforementioned peaks, the behavior of this region during sputter etching,^{7,32,35} and the relative sizes of the regions, we speculate that the principal peak in this region, peak 4, results primarily from nonbonding O(2p) orbitals that are associated with the aluminate part of these zeolites. Based upon these results and our analysis of the general behavior of the leading edges of these valence bands, we also are reasonably certain that a fairly extensive quantity of nonbonding O(2p) from the (silica and mixed silica-aluminate) balance of the zeolite overlap into this region. In fact, for NaA, this region may exhibit a shoulder peak on the high binding energy side of 4 that may also represent the *major* nonbonding contribution from the silica portion of that zeolite. Since Lowenstein's rule requires alternating Si-O and Al-O units, this near-uniting of the two nonbonding subbands seems appropriate.

B. Group II Zeolites and Their Comparison to Those of Group I: Structural Considerations. The dramatic change in valence band structure that takes place between mordenite and the A, faujasite, and L systems (the latter referred to as group I) suggests that in detecting these features the ESCA may be revealing more than just another degree of enhancement of the [Si/Al] ratio. We know, for example, that the ESCA valence band pattern for

mordenite closely resembles that for silicas, whereas those of *all* group I systems do not. We also know that in addition to the increase in the [Si/Al] ratio, mordenite represents a dramatic change in structural type from the relatively similar group I systems.

Thus, the zeolite framework for A and the faujasite systems are *cage*-like structures formed from combinations of the (β) truncated octahedron sometimes labeled as a sodalite structure. These basic units are in turn united into larger truncated cuboctahedral *cages*, sometimes labeled as α .¹ In the L system, different types of cages, called 11-hedron, or ϵ , are formed, but the operative phrase seems to be that all of these systems are structured as *interlaced cages*.

As Breck has pointed out,¹ the mordenite-zeolite system, on the other hand, is structured from linked five-ring *chains*, rather than cages. An interlaced chain-type structure is more consistent with that for the many silica-type systems, such as α -quartz and β -cristobalite, that are known to produce a valence band spectrum similar to that of mordenite, for example, like the one in Figure 6a.

It is possible that these points may suggest a strong structural (as opposed to chemical) reason for the dramatic change in the configuration of the valence band for mordenite compared to the group I zeolites. One may, however, also employ an alternative argument, based primarily on composition, to explain at least part of the change. The latter is centered around the Lowenstein rule that basically requires maximum alternation of (a) and (b) in any (a)-(b) (e.g., SiO₂-AlO₂⁻) system.¹ This rule has, in the past, been assumed to apply specifically to NaA, but may also have more general applicability to most zeolite systems. If the rule is rigorously realized, it would produce easy to discern relationships for the atomic environment around each oxygen in a zeolitic framework. Thus, for a "Lowenstein" NaA (assumed to have [Si/Al] = 1!) no oxygen is bonded exclusively to either two Si or two Al atoms, whereas in the case of Lowenstein dominated X, Y, and L systems, increasing percentages of oxygens are bonded continuously to two or more silicons. But, interestingly, only when one gets to the mordenite system does the Lowenstein rule make it possible for immediately adjacent oxygen to experience the relatively large direct (adjacent) repulsion from other oxygens that are bonded only to silicons, i.e., completely free from bonding to an aluminum atom.

Because of the relatively close packing of the oxygens in the zeolite lattice, the repulsion experienced by neighboring oxygens must influence the energetic structure of the zeolite valence band at least within an order of magnitude of the influence exerted by the bonding of the oxygens to the silicons or aluminums. This suggests that for the systems under consideration, only when one reaches mordenite is that repulsion countered *only* by Si-O bonding.

In view of the latter suppositional argument, one might be inclined to ascribe the detected change in valence band structure experienced by mordenite (compared to the group I zeolites) to chemical compositional, rather than structural, factors.

It is probable, however, that both structural and chemical arguments contribute to the substantial variation in valence band structures, with, as stated above, both differences in [Si/Al] ratios and bonding characteristics playing major roles. In fact, it is obvious that these loosely formed suppositions must await careful band structure calculations and higher resolution experimental results before any firm conclusions may be drawn.

It should be noted that certain features of the *absolute* nature of the Lowenstein rule for zeolites were recently challenged. In the latter, it was argued that there may be evidence for some -Al-O-Al- type linkages in A zeolites,¹⁶ and their existence was suggested on both structural^{40,41} and quantum mechanical^{16,41} grounds. These suggestions were, however, persuasively countered, and arguments in support of the Lowenstein rule seem now to be

(40) Smith, J. V. *Feldspar Minerals*; Springer Verlag: New York, 1974; Vol. 1, p 79. Senderov, E. E. *Phys. Chem. Miner.* **1980**, *6*, 251.

(41) See, for example: Bursill, L. A.; Lodge, E. A.; Thomas, J. M. *Nature (London)* **1981**, *291*, 265.

on sound footing.⁴² Thus, it seems reasonable to argue that these rules play a part in our results, but we cannot determine the extent.

An alternate way of considering the aforementioned adjacent oxygen proposition would be to fix on a particular silicon or aluminum site, M, and note that this site is chemically attached to four oxygens which, in turn, are attached to four additional Si or Al sites, M'. Each of the latter sites are further attached to three other oxygens, each of which is attached to an additional Si or Al site, M''. It should be apparent that radiating out from the original (M) site we have designated 1, 4, and 12 primary, secondary, and tertiary Si and Al sites. If our central site (M) contains an aluminum, then (according to Lowenstein's rule) for all zeolites, all M' must be Si. In the case of NaA, this then requires that all M'' be filled by Al. It is, therefore, not hard to discern why NaA is extensively altered from silica in its bonding chemistry. It is further apparent that if one assumes maximum dispersion of Al's (a probable statistical feature not explicitly required by the Lowenstein rule), then NaY will also exhibit some presence of aluminum in every M'' triplet set. This is obviously not true for the zeolites from mordenite through silicalite, where extensive (-Si-O-Si-) silica-like units may, for the first time, occur. If one examined the resulting structures, it would not be hard to demonstrate that if Lowenstein's rule is maintained, the zeolites from types A to L should always have at least one Al in each of the M or M' groups. Mordenite, however, should have alternating cases with only silicons present in M, and M', and the percentages of arrays with only Si should increase linearly with the increase in the [Si/Al] ratio.

The last argument may, like the first, be viewed as a structural consideration, but whether one views the reason as structural or chemical, it would appear that several factors must contribute to making the valence band spectrum for mordenite significantly different from those exhibited by zeolites with smaller [Si/Al] ratios.

C. Use of Persistence and Amalgamation Arguments To Describe Zeolite Valence Bands. As we have stated, it is not unreasonable to visualize certain aspects of the zeolites under consideration in this paper as suggestive of silica, with tetrahedrally oriented metal aluminates substituted into the silicate lattice. This loosely implies the concept of a solid, binary, substitutional solution. The latter seems particularly feasible since the resulting zeolite compounds bracket nearly every conceivable composition, similar to the phase relationship of a complicated alloy. This, in turn, suggests that one might speculate about the types of quasi-mixed crystalline solutions formed, and adjudge these somewhat loosely, employing arguments already developed by Onodera and Toyozawa³⁷ (O-T) (for unrelated binary systems). The latter suggests that certain aspects of the spectroscopy of mixed crystals may be classified in terms of two basic categories: *persistent* and *amalgamated*.

Persistence is suggested when two optical peaks are found for a binary system at or near the corresponding transition points for the two pure substances, whereas amalgamation occurs when the spectra of the two pure substances seem to coalesce into one (intermediate) peak. Theoretically, it has been argued that the existence of these two cases depends upon the difference, Δ , in an optical transition energy for the two individual components, T , the widths of their valence bands, and, C , the concentration of one of the species (the solute) dissolved in the matrix of the other (the solvent).

If we assume that, for our present case, the solute is NaAlO₂ and the solvent SiO₂, one finds for C (in ~ mol %): 50 (A), 42 (X), 30 (Y), 25 (L), 16 (mordenite), 4 (ZSM-5), and 1 (silicalite), where average zeolites of each type are assumed. Based upon calculations and spectroscopic observations, we have approximated T to be between 7 and 11 eV, whereas Δ , the difference between the atomic excitation energies of pure SiO₂ and AlO₂⁻, has been estimated at ~3 eV. Thus, for these zeolites, the critical ratio, Δ/T , defined by O-T,³⁷ is assumed to be ~0.35. These arguments

and the resulting value should be consistent with results obtained employing either perturbation theory or Green's functions through the virtual crystal limit.⁴³ *This result suggests that the zeolites in question should exhibit a pattern typical of an amalgamation-type electronic structure for all concentrations, except relatively dilute solutions.*

Since the spectroscopic transitions described by Onodera and Toyozawa are not those being considered herein, it is not immediately obvious how to proceed with this argument. However, a reasonable guess would be to assume that those ESCA transitions that are common to both SiO₂ and NaAlO₂, e.g., the O(1s), should exhibit a singular, perhaps somewhat broadened, peak for systems like the A, Y, and L zeolites, and that is indeed what we observe.⁶⁻⁸ In addition, the valence band density of state for A → L should also be a relatively straightforward sum of the bands of the two separate components (SiO₂ and NaAlO₂). The group I valence bands do suggest a mixture of contributions from both components, but the generated spectra are far from straightforward sums. In fact, as described above, the bands detected suggest several fairly complex contractions of the individual densities of states, with particularly the O(2p) region that is stabilized by the Si(3s) and Si(3p) collapsed into the middle of the band.

This may not entirely destroy the utility of the persistence/amalgamation argument, but, at least, it suggests an extensive perturbation of that, somewhat simplified, proposal. This perturbation should result from the fact that in the present case there is the formation of specific intermetallic (zeolite) subcompounds, rather than just simple binary alloy substitution. In fact, scrutiny of the terms included in the theoretical arguments of O-T³⁷ indicate that none of these terms properly deals with any of the *changes in covalent or ionic bonding that must occur during zeolite formation*. In a subsequent publication, theoretical arguments will be presented that suggest that inclusion of representations of these bonding effects will produce the resulting band contractions as perturbations inside the O-T formulation.

The situation with the zeolites of relatively large [Si/Al] ratio, e.g., mordenite → silicalite, is obviously somewhat different. Based upon the arguments of O-T, the present results suggest that, in the range above 80% silica, there is some type of transition, where the previously described (perturbed) amalgamation system seems to become more closely associated with the intermediate case defined by O-T, where the species of relatively low concentration (NaAlO₂) acts like an impurity dopant in the lattice of the predominant solvent species (SiO₂). This suggests that for zeolites with Al mole fractions of less than 20% of the total [Si] + [Al], the valence band should resemble silica with a particular perturbation. This, of course, is what is detected for mordenite, Figure 6a, where the perturbation is suggestive of that expected for NaAlO₂. According to the O-T arguments, as the [Si/Al] ratio increases from mordenite, the aluminate perturbation should separate spectroscopically from the silica valence band until it forms a distinct entity of its own. This may occur around the concentration of silicalite; however, at this concentration of NaAlO₂, the sensitivities of the present spectrometers are too poor to detect this effect. (One may, in fact, wish to argue that our previously reported⁸ detection of the presence of alumina and aluminate impurities in mordenite, ZSM-5, and silicalite is a manifestation of this spectroscopic separation.)

In summary, it would appear that the concept of viewing the electronic structure of zeolites as representative of the effects of considering those species to be amalgamated binary solid solutions of silica and sodium aluminate has some potential merit, but may be of real value only if (in the appropriate quantum argument) additional terms are considered that introduce proper bonding effects into the perfect periodicity/virtual crystal model.

VI. Summary

The first detailed experimental ESCA study of the valence band spectra of numerous silica-aluminate zeolites has been presented. Based upon the general features of these spectra we have sub-

(42) Bennett, J. M.; Blackwell, C. S.; Cox, D. E. *J. Phys. Chem.* **1983**, *87*, 3783.

(43) Jones, W.; March, N. H. *Theoretical Solid State Physics*; Dover: New York, 1985; Vol. 2.

divided the zeolites into two, somewhat artificial, classes: group I, systems of [Si/Al] ratios from 1 to 3, typified by structures dominated by interlaced tetrahedral silica aluminate cages, e.g., A, X, Y, and L zeolites; and group II, systems of large [Si/Al] ratio from 5 to > 100, typified by structures dominated by interlaced chains, e.g., mordenite, ZSM-5, and silicalite.

The valence band spectra exhibited by these zeolite systems are *not* just additive renditions of that for silica and for alumina, but rather the zeolite spectra reveal complex shiftings and alterations.

In addition, the valence band results for the group II systems appear to be quite similar in appearance to silica, suggesting a silica-dominated system with increasing aluminate perturbation as the [Si/Al] ratio decreases, i.e., silicalite < ZSM-5 < mordenite. There is a rather abrupt and not entirely understood change in the detected valence band structure after mordenite, as the [Si/Al] ratio decreases, perhaps suggesting a recognition by the ESCA of a difference between the aforementioned chain-like structures with large [Si/Al] (II), compared to the cage-like structures with [Si/Al] ratios between 3 and 1 (I).

The valence band results for all of the group I zeolites are shown to produce three principal subband regions, with a number of peaks detected in each. Based upon a variety of results, calculations, and other supportive information, suppositional identifications are made of each of these peaks. In this manner, the bonding and nonbonding character of these zeolites are broken down, analyzed, and compared. It is suggested, for example, that the relative ionicity (polarity) of the zeolites increases inversely with the

[Si/Al] ratio, with the silica covalency of the NaA system so depleted that it seems more appropriate to describe it as a partially ionic sodium aluminate, perturbed by silica. In all cases, the subbands shift and contract dramatically from those for the "precursor" systems (silica and sodium aluminate), suggesting that the substitution of the latter into the tetrahedral silica lattice substantially perturbs the electronic structure of the silica, but does so through the interjection of *group* (NaAlO₂), rather than elemental (ESCA) *shifts*.

Suppositional arguments are presented to explain the spectral distinction between group I and II systems based on both structural and compositional factors. Lowenstein's rule is also employed, but the extent of its application is hard to determine.

Consideration is also given for the description of these materials in terms of the Green's function based amalgamation/persistence models of Onodera and Toyozawa.³⁷ It is argued that the zeolites, in question, should fall into the amalgamation category, but those in group I fail to do so properly without the inclusion of additional terms in the Green's functions to describe the covalent and/or ionic bonding that seems to prohibit the zeolites from being simple solid solutions of SiO₂ and NaAlO₂. This model does seem to provide an explanation of the valence bands of the group II zeolites based on the perturbation of the silica lattice by varying amounts of aluminate.

Useful information has also been extracted from studies of the behavior of zeolite valence bands during change of cations, selective sputter etching, catalytic abuses, thermal treatment, etc. The details of these studies are presented in other publications.^{9,11,32,35}

Characterization and Novel Low-Temperature Reactions of FeCH₂ and N₂FeCH₂

Sou-Chan Chang, Robert H. Hauge, Zakya H. Kafafi, John L. Margrave,* and W. E. Billups*

Contribution from the Department of Chemistry, Rice University, Houston, Texas 77251. Received March 21, 1988

Abstract: The reactions of iron atoms with diazomethane have been investigated in argon matrices by FTIR matrix isolation spectroscopy. These studies show that iron atoms insert spontaneously into diazomethane to yield FeCH₂ and N₂FeCH₂. Photolysis of the matrix at $\lambda \geq 500$ nm leads to the reductive elimination of iron from N₂FeCH₂. UV photolysis of the matrix results in the facile conversion of FeCH₂ to HFeCH, whereas photolysis of the carbyne through a cutoff filter with $\lambda \geq 400$ nm leads to the reverse process. FeCH₂ and N₂FeCH₂ react with dihydrogen to yield CH₃FeH and N₂CH₃FeH, respectively, with N₂FeCH₂ reacting more rapidly than FeCH₂. FeCH₂ was found to react with water to yield CH₃FeOH.

Although carbene complexes are recognized as important intermediates in a large number of catalytic reactions, only a limited number of instances have been reported in which authentic carbene intermediates have been used to initiate the catalytic cycle. In most instances this can be attributed to the short lifetime and low concentration of the intermediate. Accordingly, these systems are usually modeled using fairly stable complexes.¹ FTIR matrix isolation spectroscopy is often used to characterize unstable species present in low concentration. In this paper we describe the synthesis and characterization of FeCH₂ and N₂FeCH₂, their reactions with dihydrogen and water, and the photolytic rearrangement of FeCH₂ to HFeCH.

Experimental Section

A complete description of the multisurface matrix isolation apparatus has been reported.² The preparation of CH₂N₂, CD₂N₂, CHDN₂, and

¹³CH₂N₂ has also been discussed.³ Iron atoms (AESAR, 99.98%) were vaporized from an alumina crucible enclosed in a resistively heated tantalum furnace over the range 1300–1500 °C. The temperature of the furnace was measured with a microoptical pyrometer (Pyrometer Instrument Co.).

In a typical experiment, iron atoms and diazomethane were cocondensed with argon (Matheson, 99.9998%) or nitrogen (Matheson, 99.9995%) onto a rhodium-plated copper surface at 11–14 K over a period of 30 min. Prior to deposition, the molar ratio of iron, diazomethane, and matrix gas was measured with a quartz crystal microbalance mounted on the cold block. During deposition the rate of effusion of iron was continuously monitored with a water-cooled quartz crystal microbalance situated at the back of the furnace. In this study the molar ratio of iron to matrix gas was varied from 0 to 23 parts per thousand and the ratio of diazomethane to matrix gas was varied from 0 to 15 parts

(2) Hauge, R. H.; Fredin, L.; Kafafi, Z. H.; Margrave, J. L. *Appl. Spectrosc.* **1986**, *40*, 588.

(3) Chang, S.-C.; Kafafi, Z. H.; Hauge, R. H.; Billups, W. E.; Margrave, J. L. *J. Am. Chem. Soc.* **1987**, *109*, 4508.

(1) See: *Transition Metal Carbene Complexes*; Verlag Chemie: Weinheim, 1983.